REPORT

POLYMER CHEMISTRY

Polyethylene upcycling to long-chain alkylaromatics by tandem hydrogenolysis/aromatization

Fan Zhang[1]*, Manhao Zeng[2]*, Ryan D. Yappert[3], Jiakai Sun[2], Yu-Hsuan Lee[2], Anne M. LaPointe[4], Baron Peters[3], Mahdi M. Abu-Omar[1,2], Susannah L. Scott[1,2]†

The current scale of plastics production and the accompanying waste disposal problems represent a largely untapped opportunity for chemical upcycling. Tandem catalytic conversion by platinum supported on γ-alumina converts various polyethylene grades in high yields (up to 80 weight percent) to low-molecular-weight liquid/wax products, in the absence of added solvent or molecular hydrogen, with little production of light gases. The major components are valuable long-chain alkylaromatics and alkylnaphthenes (average ~C_{30}, dispersity $Đ$ = 1.1). Coupling exothermic hydrogenolysis with endothermic aromatization renders the overall transformation thermodynamically accessible despite the moderate reaction temperature of 280°C. This approach demonstrates how waste polyolefins can be a viable feedstock for the generation of molecular hydrocarbon products.

Over the past 70 years, global production of synthetic, petroleum-based plastics has risen sharply, from less than 2 million tonnes in 1950 to 380 million tonnes in 2015 (*1*). Production is projected to double again within the next 20 years (*2*). Plastics have become indispensable in many facets of modern life, enhancing the security of our food and health care systems, the performance of textiles, the versatility of consumer electronics, and the energy efficiency of transportation. About 40% of these plastics are destined for short-term use, and most (>90% in the United States) are not recycled (*1*). The vast bulk of this plastic waste ends up in landfills or is incinerated. However, the embodied energy that can be recovered by combustion is far less than that used in the original manufacturing of the plastic (*3*). Furthermore, a substantial fraction of the waste is mismanaged, ending up in rivers and oceans where its chemical inertness leads to extremely slow degradation and visible accumulation in the natural environment (*4*, *5*).

Efforts to develop closed-loop life cycles for synthetic plastics by relying on collection, separation, and mechanical recycling have had limited success. The inferior properties of the recycled materials, relative to virgin plastics, contribute to the economic challenges of the "downcycling" model (*6*). New types of polymers that degrade rapidly in the environment are being investigated (*7*), although such materials do not currently have either the physical properties or the cost structure to displace existing commodity plastics. Degradable plastics can also contaminate recycling streams and may encourage single-use product design. Depolymerization (also known as chemical or feedstock recycling) can recover the original monomer subunits, repolymerization of which yields materials with properties identical to those of the original plastic (*8*). However, this strategy requires prohibitive amounts of energy for polyolefins such as polyethylene (PE) and polypropylene (PP). Controlled partial depolymerization could convert post-consumer waste plastics directly into more valuable chemicals ("upcycling"), although few such processes have yet been developed.

High- and low-density polyethylenes (HDPE and LDPE) currently represent the largest fraction (36% by mass) of all plastic waste (*1*). Their depolymerization by pyrolysis at temperatures above 400°C, with or without a catalyst, generates complex, low-value mixtures of gas, liquid hydrocarbons, and char (*9*, *10*). Somewhat more selective disassembly can be achieved at lower temperatures via catalytic hydrogenolysis (*11*, *12*) or tandem catalytic alkane metathesis (*13*), but the low-value alkane products are unlikely to recoup the costs of recovery, separation, and processing using large amounts of a co-reactant (H_2 or liquid alkanes, respectively).

Aromatics are more attractive target products from partial depolymerization. The conventional process for making aromatics is naphtha reforming. This energy-intensive process generates a mixture known as BTX (benzene-toluene-xylenes) at 500° to 600°C (*14*). In a subsequent step with a large environmental footprint, BTX is alkylated to give linear alkylbenzenes (LABs, used for making surfactants). The most widely used processes require linear olefins (typically, C_{10} to C_{16}) and liquid HF or $AlCl_3$-HCl as the acid catalyst (*15*). Manufacturing the BTX by aromatization of shale gas–derived light alkanes requires harsher reaction conditions (propane, 550° to 700°C; ethane, 600° to 800°C; methane, 900° to 1000°C) (*16*), and the catalysts tend to deactivate rapidly. New zeolite-based catalysts can transform either methanol (*17*) or syngas (*18*) into BTX aromatics at lower temperatures, 300° to 400°C. Biomass-based routes include oxidative coupling of ethanol to aromatic alcohols and aldehydes (*19*), hydrogenolysis/hydrodeoxygenation of bio-oils or lignin to give propylbenzene (*20*), and Diels-Alder reactions of carbohydrate-derived furanics to give *p*-xylene (*21*). However, slow rates, low yields, and high H_2 requirements make these processes expensive to operate, and none are practiced commercially. BTX is also formed in the catalytic pyrolysis of PE at 400° to 600°C, although deactivation of the zeolite catalysts by coking is severe (*22*). The yields are moderate (up to 50 wt %), and large amounts of low-value gases (C_1 to C_5, > 50 wt %) are formed. Conventional and proposed routes to BTX and linear alkylaromatics are compared in Fig. 1.

Here, we report a one-pot, low-temperature catalytic method to convert various grades of PE directly to liquid alkylaromatics over a simple heterogeneous catalyst. In a proof-of-concept experiment, a low-molecular-weight PE (0.118 g, $M_w = 3.5 \times 10^3$ g mol^{-1}, $Đ$ = 1.90) was combined with Pt/γ-Al_2O_3 (0.200 g, containing 1.5 wt % Pt dispersed as ~1-nm nanoparticles; fig. S1, A and B) in an unstirred mini-autoclave (internal volume 10 ml) without solvent or added H_2 (Fig. 2A). After 24 hours at 280° (±5)°C, the liquid/wax products (80% by mass) were recovered for characterization by dissolving in hot $CHCl_3$ (Fig. 2B, experiment 1). According to gel permeation chromatography with refractive index detection (GPC-RI), most of the PE underwent a decrease in M_w by nearly a factor of 10, to 430 g mol^{-1}, as well as the expected (*23*) decrease in dispersity (to $Đ$ = 1.31). On the basis of their orange color and the appearance of ^{1}H nuclear magnetic resonance (NMR) signals in the region 6.5 to 9.0 ppm (fig. S2), these hydrocarbons appear to have substantial aromatic content. The $CHCl_3$-insoluble solids include a small amount of organic residue (~5 wt %) in addition to the catalyst. The former includes unreacted polymer and large oligomers (including less soluble alkylaromatics), as judged by infrared and ^{1}H NMR spectroscopy (figs. S3 and S4). The missing mass (~15 wt %) is presumably volatile hydrocarbons and gases, which were not collected in this exploratory

[1]Department of Chemical Engineering, University of California, Santa Barbara, CA 93106, USA. [2]Department of Chemistry and Biochemistry, University of California, Santa Barbara, CA 93106, USA. [3]Department of Chemical Engineering, University of Illinois, Urbana-Champaign, IL 61801, USA. [4]Department of Chemistry and Chemical Biology, Cornell University, Ithaca, NY 14583, USA.
*These authors contributed equally to this work.
†Corresponding author. Email: sscott@ucsb.edu

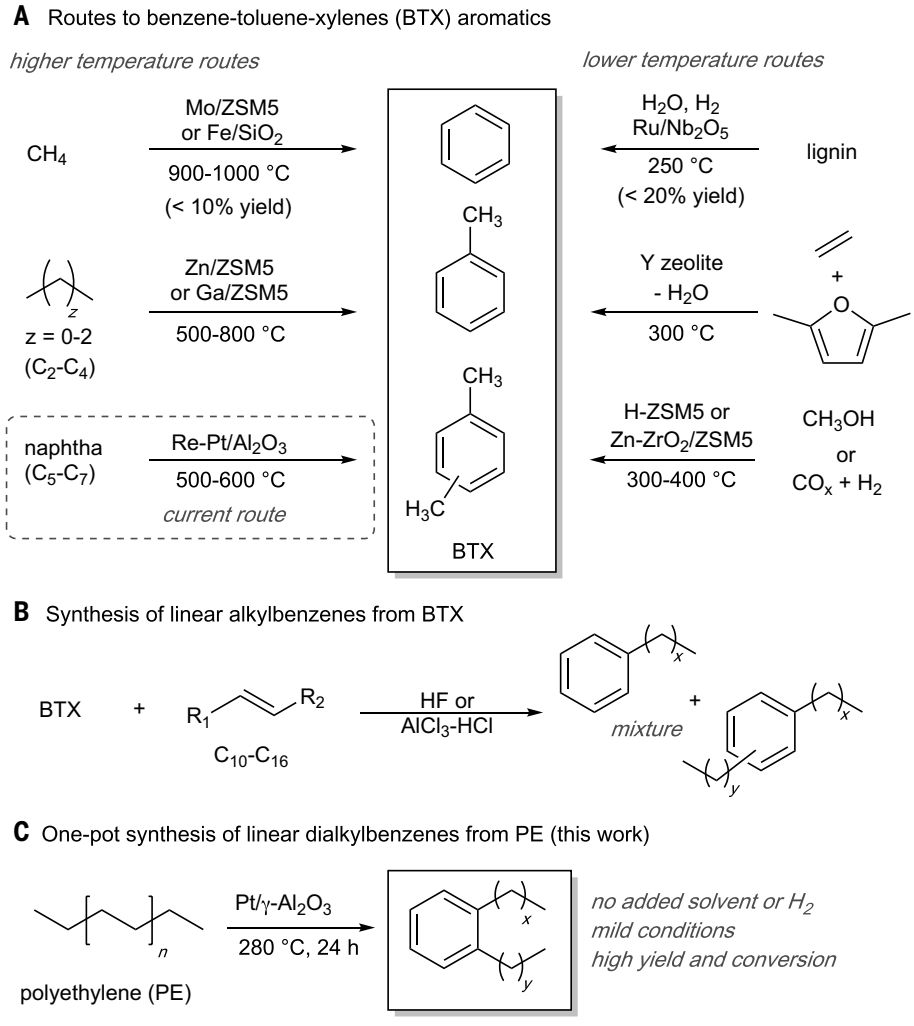

Fig. 1. Routes to alkylbenzenes. (**A** to **C**) Current and proposed routes to BTX (A) and the current downstream transformation of BTX to linear alkylbenzenes (B) are compared to the one-pot tandem process from polyethylene (C) reported here.

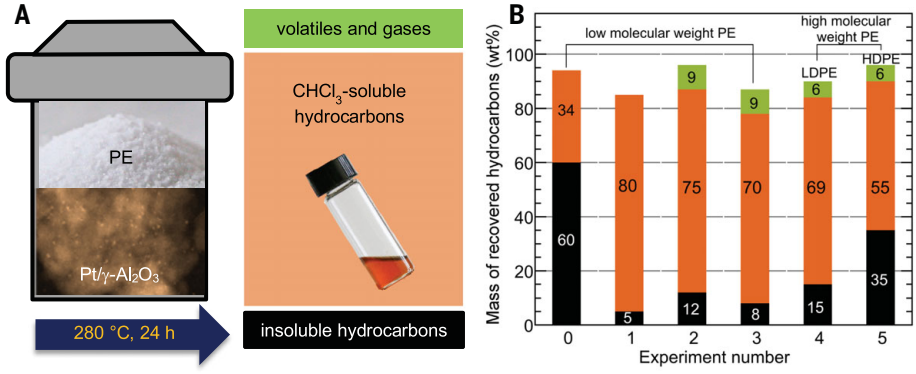

Fig. 2. Solvent-free conversion of various types of polyethylene. (**A**) Schematic of reactor and product fractions, with photographs of the powdered polymer and liquid products, as well as a transmission electron micrograph of the catalyst. (**B**) Hydrocarbon distributions after 24 hours at 280°C. Reactions of a low-molecular-weight PE (M_w = 3.52 × 10^3 g mol^{-1}, $Đ$ = 1.90) in an unstirred mini-autoclave reactor: (0) catalyzed by γ-Al_2O_3 (no gas recovery); (1) catalyzed by Pt/γ-Al_2O_3 (no gas recovery); (2) catalyzed by Pt/γ-Al_2O_3 (with gas recovery). Reactions catalyzed by Pt/γ-Al_2O_3 in a stirred autoclave reactor with gas recovery: (3) low-molecular-weight PE; (4) LDPE bag (M_w = 9.45 × 10^4 g mol^{-1}, $Đ$ = 7.37); (5) HDPE bottle cap (M_w = 5.35 × 10^4 g mol^{-1}, $Đ$ = 3.61).

experiment. In a control experiment conducted without the catalyst under the same reaction conditions, the PE showed no appreciable decrease in M_w. A second control experiment using the same amount of γ-Al_2O_3 but without Pt resulted mostly in a $CHCl_3$-insoluble residue (~60 wt %) and a much lower yield of soluble hydrocarbon products (34 wt %), with a smaller decrease in molecular weight (M_w = 1421 g mol^{-1}, $Đ$ = 1.85) and negligible aromatic content (Fig. 2B, experiment 0).

To obtain a more complete mass balance and to characterize the volatile reaction products, the exploratory experiment was repeated in a mini-autoclave equipped with a gas port. The recovered gases represent a small fraction of the original polymer mass (9 wt %). They include H_2 (0.2 mg, quantified by GC-TCD) and light hydrocarbons (C_1 to C_8, 9.8 mg, quantified by GC-FID) (figs. S5 and S6). The latter were primarily methane, ethane and propane, with minor amounts of *n*-hexane, cyclohexane, methylcyclopentane, benzene, and *n*-heptane. Additional volatile hydrocarbons (C_7 to C_{11}, 1.5 mg) were recovered by distillation from the autoclave at 150°C. Their major component was toluene (47 wt %). Together, the light hydrocarbons, the $CHCl_3$-soluble liquids/waxes (89 mg) and the insoluble organic residue (14 mg) represent an overall mass balance of 96% (Fig. 2B, experiment 2).

When the reaction was conducted in a larger, stirred autoclave (internal volume 90 ml), most of the PE (70 wt %) was converted at 280°C to high-boiling liquids/waxes (Fig. 2B, experiment 3). In this case, the waxes (24 wt %, M_w = 723 g mol^{-1}, $Đ$ = 1.34) separated spontaneously from the liquids (46 wt %, M_w = 520 g mol^{-1}, $Đ$ = 1.12) inside the reactor. GPC analysis of the liquid fraction using both RI and ultraviolet (UV) detection gave similar results (Fig. 3A), demonstrating that the UV-active (i.e., aromatic) chromophores were evenly distributed across the molecular weight range. The ^{13}C NMR spectrum contains signals in the aromatic region (120 to 150 ppm), most corresponding to unsubstituted ring carbons (Fig. 3B). The ^1H NMR spectrum shows that most aromatic protons are associated with benzene rings (6.5 to 7.4 ppm), with fewer bonded to fused aromatic rings such as naphthalenes (7.4 to 9.0 ppm) (*24*). There is no evidence for olefins or dienes (4.5 to 6.5 ppm; fig. S8A).

The high yield of liquid alkylaromatics was particularly promising; such compounds find widespread application as surfactants, lubricants, refrigeration fluids, and insulating oils (*25*), and their manufacture from waste polyethylene could displace fossil fuel–based routes. The ^1H NMR spectrum reveals more information about the alkyl substituents (fig. S8A). Protons associated with an aliphatic carbon

directly bonded to an aromatic ring (C_α) resonate in the region 2 to 4 ppm. The overall ratio $H_\alpha/H_{aromatic}$ = 1.1 indicates that the major species are, on average, dialkylaromatics (figs. S7 and S8A). This finding is consistent with a previous report in which dialkylbenzenes were the major products of catalytic aromatization of lighter *n*-alkanes (C_6 to C_{12}) (*26*), and with their proposed mechanism of formation by dehydrocyclization of polyethylene (Fig. 4). Combining this information with the overall fraction of aromatic protons (0.037) and the average carbon number (C_{34} for this experiment, based on the M_n value determined by GPC), we estimate the overall alkylaromatic selectivity in the liquid fraction to be 57 (±5) mol %, of which ~40 mol % is monoaromatic (table S3, experiment 3). Using the aromatic carbon fraction (0.10 according to ^{13}C NMR; fig. S8B) instead results in a similar estimate for the alkylaromatic selectivity, 52 (±4) mol %. Furthermore, many of the alkyl substituents are unbranched at the C_α position, judging by the intense ^1H signals at 2.35 to 2.85 ppm. The paraffinic $-CH_2-/-CH_3$ ratio, 7.5, suggests that each alkyl substituent possesses, on average, < 1 branch point.

Individual molecular components in the liquid fraction were identified using field desorption–mass spectrometry (FD-MS; fig. S9). Each mass series shows a log-normal distribution with a maximum intensity at ~C_{30} (fig. S10). The most abundant products are the alkylbenzene series (14*n* – 6, ~22 mol %), as shown in Fig. 3C. Saturated alkanes and alkylnaphthalenes share the same mass profile (14*n* + 2, 20 mol %) and are the next most abundant group, with smaller amounts of alkyltetralins (14*n* – 8, 16 mol %) and alkylnaphthenes (i.e., alkylcycloalkanes; 14*n*, 17 mol %). Alkylnaphthalenes presumably arise by further dehydrocyclization of alkylbenzenes (Fig. 4) (*27*). Minor aromatic products include polyaromatics such as alkylanthracenes and alkylphenanthrenes (14*n* – 4, 7 mol %) and their partially hydrogenated analogs (14*n* – 10, 8 mol %). According to FD-MS, the selectivity for monoaromatic products (including both alkylbenzenes and alkyltetralins) is ~40 mol %, consistent with the ^1H NMR analysis described above. The alkylnaphthene products, which have intrinsic value as solvents and hydrogen donors (*28*), could be further dehydrogenated to alkylaromatics by active control of the partial pressure of H_2 in the reactor. The total yield of cyclic products (both alkylaromatics and alkylnaphthenes) in the liquid products is 88 mol % (table S4).

When the reaction time was extended from 24 to 36 hours at 280°C, similar products were formed (table S3, experiment S1), although the molecular weight distributions of both liquid and wax fractions shifted to slightly lower values (fig. S11) and the dispersity decreased further (to $Đ$ = 1.06). At the same time, the alkylaromatic selectivity increased (24 hours, 52 and 71 mol %, respectively, in the liquid and wax fractions; 36 hours, 70 and 88 mol %, respectively) (table S3). Alkylaromatic yields were also strongly temperature-dependent. After 24 hours at a lower temperature (250°C), the $CHCl_3$-soluble hydrocarbons (13 wt %) showed a smaller extent of depolymerization (M_w = 1.8 × 10^3 g mol^{-1}, $Đ$ = 2.11) and negligible aromatic content; most PE was simply not converted. At a higher reaction temperature (330°C), the polymer was largely converted in 24 hours; however, the major products (77 wt %) were gases and volatile hydrocarbons. The yield of $CHCl_3$-soluble hydrocarbons was low (~10 wt %), although the overall yield of aromatics was higher ($H_{aromatic}/H_{total}$ = 0.38), with more

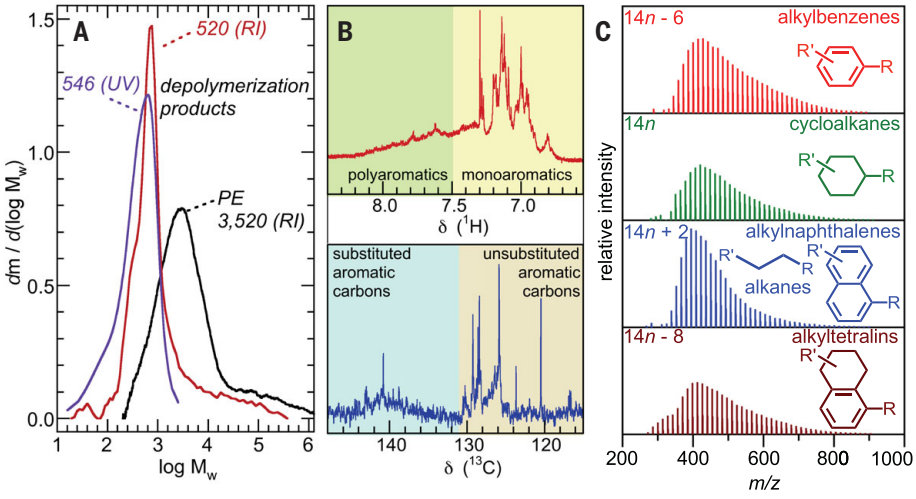

Fig. 3. Analysis of the liquid hydrocarbon fraction from the solvent-free catalytic conversion of polyethylene. Sample had M_w = 3.52 × 10^3 g mol^{-1} and was heated for 24 hours at 280°C (Fig. 2B, experiment 3). (**A**) GPC analysis, conducted using both RI and UV detectors. (**B**) ^1H and ^{13}C NMR spectra, recorded in deuterated TCE. (**C**) FD-MS analysis.

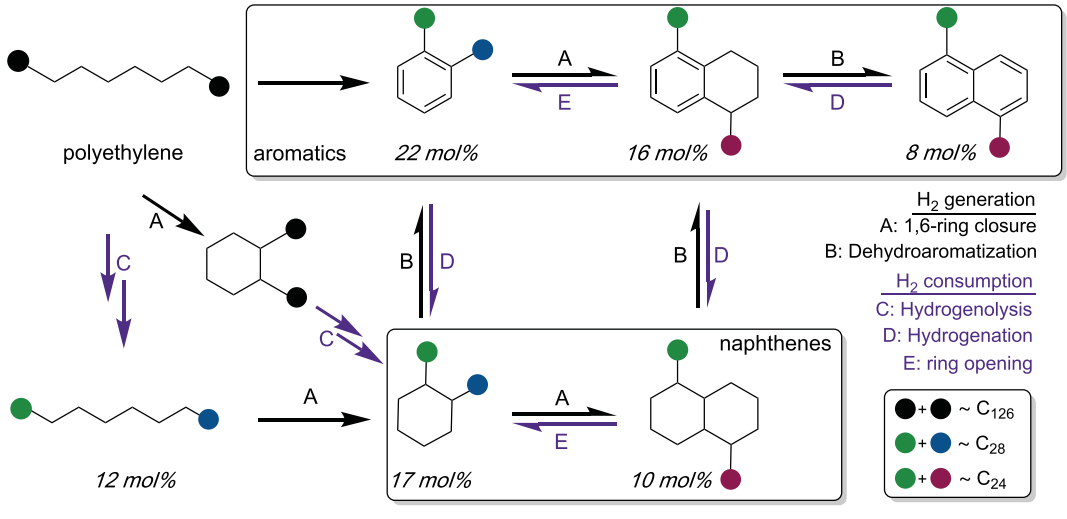

Fig. 4. Overall PE conversion to alkylaromatics and alkylnaphthenes, and proposed mechanism of tandem polyethylene hydrogenolysis/aromatization via dehydrocyclization. Yields of each product were estimated using a combination of ^1H NMR and FD-MS analysis (see supplementary materials and tables S2 and S4).

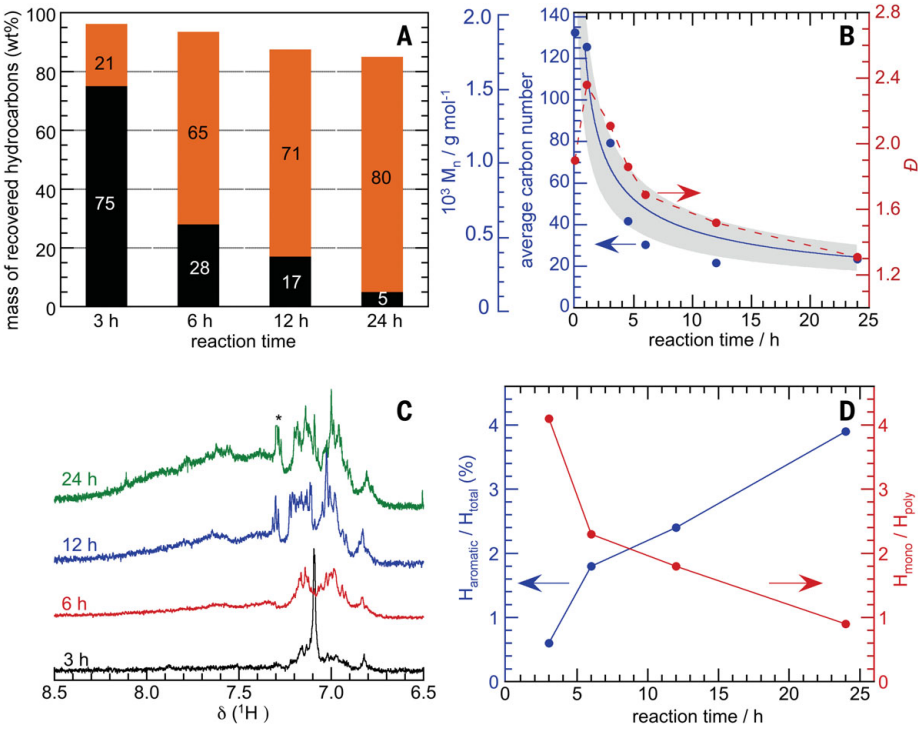

Fig. 5. Time course of the solvent-free disassembly of polyethylene (M_n = 1.85 × 10^3 g mol^{-1}; $Đ$ = 1.90) catalyzed by Pt/γ-Al_2O_3 in an unstirred mini-autoclave reactor at 280°C. (**A**) Evolution of major product fractions (orange, $CHCl_3$-soluble liquids/waxes; black, insoluble hydrocarbons). (**B**) Overall molecular weight (M_n, blue) and dispersity ($Đ$, red) for all non-gas hydrocarbons. The red dashed line is present only to guide the eye. The curve fit (solid blue line) shows the refinement of Eq. 3 to the M_n data. Initial conditions: total carbon n_C = 8.4 mmol; number of polymer chains N_0 = 68 μmol; total Pt m_{Pt} = 3 × 10^{-3} g; selectivity for aromatization versus hydrogenolysis, s = 1/2 (eq. S22). The shaded region indicates the 95% confidence bands for the model fit. Each independent measurement, which may diverge from the fit because of measurement error, has a 95% confidence interval that represents the mean of many measurements. The set of confidence intervals at all reaction times represents the confidence bands in which the true fit, given the form in Eq. 3, lies. Because the fit and its confidence bands predict the mean of many measurements at a given reaction time, individual measurements can lie outside these bands. (**C**) Time course of the ^{1}H NMR spectra of the liquid/wax fraction in the aromatic region. The asterisk indicates a truncated residual solvent signal. (**D**) The fraction of aromatic protons and the ratio of mono- to polyaromatic protons.

polyaromatics (H_{mono}/H_{poly} = 0.25). The optimum temperature for alkylbenzene formation is therefore 250°C < T < 330°C.

The time course of PE depolymerization was studied at 280°C (table S5, experiments 1a to 1g). A short induction period, lasting about 1 hour, corresponds in large part to the time required for thermal equilibration of the reactor (~0.75 hours). After this time, the liquid hydrocarbon fraction increased (Fig. 5A) as M_n decreased, eventually approaching a plateau at 315 g mol^{-1} after ~6 hours (Fig. 5B). The dispersity $Đ$ increased initially from 1.94 to 2.36, then decreased to stabilize at 1.31. The alkylaromatic yield also changed appreciably over the course of the reaction. After 3 hours, aromatic protons represented <1% of all protons, mainly associated with alkylbenzenes (Fig. 5, C and D). At longer reaction times, the aromatic fraction and the yield of alkylnaphthalenes increased (table S5).

We also assessed the thermodynamics of n-alkane aromatization. The temperature needed to achieve appreciable aromatic yields for this endothermic reaction (Eq. 1) decreases as the molecular weight increases (*29*).

$$C_mH_{2m+2} \rightarrow C_mH_{2m-6} + 4H_2 \qquad (1)$$

Nonetheless, direct PE conversion to aromatics appears to require particularly mild conditions relative to the much higher operating temperatures generally required for making BTX from molecular n-alkanes (Fig. 1). Thermodynamic values for converting linear PE chains to alkylaromatics at 280°C in 1 atm H_2, estimated using Benson group contributions for long-chain n-alkanes (*30*), are ΔH_1° = 246 kJ/mol and ΔG_1° = 31 kJ/mol. Thus, aromatization alone is indeed disfavored. However, the reaction occurs in tandem with hydrogenation of a suitable hydrogen acceptor. In solvent-less PE depolymerization, the PE chains themselves serve as an internal hydrogen sink (Fig. 4). Using Benson group contributions again, the estimated thermodynamic values for C-C bond hydrogenolysis (Eq. 2) are ΔH_2° = −49 kJ/mol and ΔG_2° = −74 kJ/mol.

$$C_{m+n}H_{2(m+n)+2} + H_2 \rightarrow C_mH_{2m+2} + C_nH_{2n+2} \qquad (2)$$

Consequently, aromatization becomes favorable at 280°C (ΔG° = 0) when even 10% of the H_2 generated is consumed in PE hydrogenolysis.

On the basis of alkylaromatic yield, the aromatization in experiment 2 of Fig. 2B generated 0.50 mmol H_2. More than 90% of this H_2 (0.47 mmol) was consumed in reducing the molecular weight of the polymer via hydrogenolysis, making the tandem process thermodynamically favorable. However, the residual H_2 found in the reactor headspace at the end of the reaction (0.11 mmol) exceeds the expected value (0.03 mmol). Therefore, a significant amount of H_2 is generated in other reactions, such as PE dehydrocyclization to give cycloalkanes and tetralins. Both were observed by FD-MS (see above). Indeed, their yields are higher than the thermodynamic predictions, which favor aromatics. We observed that some of these more saturated compounds condense outside the autoclave's heated zone where the catalyst is located, thereby preventing their further dehydrogenation.

To explore whether polyethylene is necessary to produce long-chain alkylaromatics by tandem catalytic hydrogenolysis/aromatization, we investigated the reaction of n-$C_{30}H_{62}$ under the same conditions (table S6, experiments S2 and S3). Compared to PE, the n-$C_{30}H_{62}$ chains experience only half as much hydrogenolysis (consuming just 0.25 mmol H_2 according to fig. S12), as expected on the basis of the chain length dependence of hydrogenolysis kinetics (*31*). Molecules in the liquid products have an average chain length of C_{20}, with low alkylaromatic content (~10 mol %). Because hydrogenolysis and aromatization occur in tandem, they must occur together. Consequently, the formation of alkylaromatics is greatly enhanced by the use of polyethylene as a feedstock.

Although there are far too many individual reactions and products to formulate a precise kinetic model, a simplified model captures the main features of the tandem reaction. We assume that the Pt surface is covered with molten PE and/or PE-derived hydrocarbons at all times, and that the hydrogenolysis turnover frequency is constant on sites not occupied by aromatic hydrocarbons. As the latter form, they adsorb more strongly than alkanes (*32*), occupying active sites and reducing the hydrogenolysis rate accordingly. We also assume that hydrogenolysis is random (i.e., all aliphatic C-C

bonds are equally likely to be cleaved) (*33*). The sole adjustable parameter, k/K, is the ratio of the rate constant for hydrogenolysis (k) and the equilibrium constant for competitive adsorption of aromatics and aliphatic chains (K) (eq. S14). Equation 3 predicts the evolution of the average chain length as a function of the reaction time, initial total carbon amount n_C, and total platinum mass m_{Pt}.

$$\ln\left[1-\frac{3}{M_n(t)}+\frac{3}{M_n(0)}\right]+\left[\frac{3}{M_n(t)}-\frac{3}{M_n(0)}\right]=-\frac{k}{K}\frac{m_{Pt}}{n_C}t \quad (3)$$

The curve fit of Eq. 3 to an experimental dataset is shown in Fig. 5B, starting with the data point at t = 1 hour (i.e., after the induction period caused by reactor heating). Assuming a preferential binding for aromatics of K = 3.2×10^6 (*32*), the hydrogenolysis rate constant k is estimated to be 6.4×10^2 $mol_{C\text{-}C}$ bonds $hour^{-1}$ g_{Pt}^{-1} at 280°C.

The stability of the Pt/γ-Al_2O_3 catalyst was investigated by conducting three consecutive 6-hour reactions (to ensure much less than full conversion), with regeneration of the recovered catalyst between each experiment (see supplementary materials). The liquid/wax yield decreased by 15 wt % in the second run but stabilized in the third run (table S6, experiments S4 to S6, and fig. S13). The activity decrease between the first and second runs was comparable to the decrease in the active Pt surface area measured by CO chemisorption, with no notable change between the second and third runs (table S6, experiments S4 to S6). Thus, the intrinsic activity of the catalyst (turnover frequency) appears to be unchanged. The average carbon number of the liquid/wax product increased between the first and second 6-hour runs (as expected because of the lower extent of depolymerization), then stabilized in the third run. Transmission electron microscopy analysis of a catalyst used for 24 hours and regenerated by calcination showed that the Pt nanoparticles increased in size slightly, from 0.8 to 1.2 nm (fig. S1, C and D). In a preliminary scale-up attempt, the amount of PE was increased by nearly a factor of 10 (to 1.1 g) while maintaining the same PE:Pt ratio and reaction conditions. After 24 hours, 0.56 g of a liquid product (M_w = 483 g mol^{-1}, $Đ$ = 1.29) with 27 mol % aromatic content was obtained (table S6, experiment S7).

To investigate how a tandem catalytic process could be deployed to convert waste polyethylene without large energy input, we also performed solvent-free depolymerization of two different commercial grades of PE: an LDPE plastic bag ($M_w = 9.45 \times 10^4$ g mol^{-1}, $Đ$ = 7.37) and an HDPE water-bottle cap ($M_w = 5.35 \times 10^4$ g mol^{-1}, $Đ$ = 3.61). These higher-molecular-weight polymers behaved similarly to the low-molecular-weight polyethylene, giving liquid/wax products with an average carbon number of ~C_{30}. After 24 hours at 280°C, the overall liquid yields were 69 and 55 wt % for LDPE and HDPE, respectively (Fig. 2B, experiments 4 and 5), with alkylaromatic selectivities of ~44 and 50 mol % (table S3, experiments 4 and 5). Thus, the extent of depolymerization is slightly lower in the same reaction time. For these higher-molecular-weight polyethylenes, the batch process generates its own highly viscous solvent as depolymerization proceeds. Recycling some of the alkylaromatic liquids to serve as solvent for the next batch may accelerate the reaction by facilitating mass and heat transport. The similar results for three very different plastics (including two commercial-grade samples of LDPE and HDPE) suggest that density, degree of branching, and common processing impurities are not major issues.

Shorter residence times should also improve the selectivity for monoaromatic hydrocarbons relative to naphthalenes, etc., and suppress the already low gas yields even further. Alkylbenzene selectivity may be further improved by active control of the partial pressure of H_2, which must be high enough to promote PE hydrogenolysis but low enough to suppress aromatic hydrogenation. Catalyst improvements in these directions will be necessary to make the tandem reaction compatible with continuous processing and, ultimately, economically viable. The alkylbenzenes with their linear side chains could be sulfonated to produce biodegradable surfactants, which are interesting as higher-value chemical products. This type of commodity polymer upcycling can result in displacement of fossil carbon–based feedstocks, while simultaneously incentivizing better management of plastic waste and recovering considerable material value that can be recirculated into the global economy.

REFERENCES AND NOTES

1. R. Geyer, J. R. Jambeck, K. L. Law, *Sci. Adv.* **3**, e1700782 (2017).
2. L. Lebreton, A. Andrady, *Palgrave Commun.* **5**, 6 (2019).
3. O. Eriksson, G. Finnveden, *Energy Environ. Sci.* **2**, 907–914 (2009).
4. J. R. Jambeck *et al*., *Science* **347**, 768–771 (2015).
5. A. Chamas *et al*., *ACS Sustain. Chem. Eng.* **8**, 3494–3511 (2020).
6. A. Rahimi, J. M. Garcia, *Nat. Rev. Chem.* **1**, 0046 (2017).
7. Y. Zhu, C. Romain, C. K. Williams, *Nature* **540**, 354–362 (2016).
8. I. Vollmer *et al*., *Angew. Chem. Int. Ed.* **59**, 15402–15423 (2020).
9. I. A. Ignatyev, W. Thielemans, B. Vander Beke, *ChemSusChem* **7**, 1579–1593 (2014).
10. S. D. Anuar Sharuddin, F. Abnisa, W. M. A. Wan Daud, M. K. Aroua, *Energy Convers. Manage.* **115**, 308–326 (2016).
11. V. Dufaud, J. M. Basset, *Angew. Chem. Int. Ed.* **37**, 806–810 (1998).
12. G. Celik *et al*., *ACS Cent. Sci.* **5**, 1795–1803 (2019).
13. X. Jia, C. Qin, T. Friedberger, Z. Guan, Z. Huang, *Sci. Adv.* **2**, e1501591 (2016).
14. M. R. Rahimpour, M. Jafari, D. Iranshahi, *Appl. Energy* **109**, 79–93 (2013).
15. C. Perego, P. Ingallina, *Catal. Today* **73**, 3–22 (2002).
16. S. R. Kanitkar, J. J. Spivey, in *Natural Gas Processing from Midstream to Downstream*, N. O. Elbashir, M. M. El-Halwagi, I. G. Economou, K. R. Hall, Eds. (Wiley, 2019), pp. 379–401.
17. I. Yarulina, A. D. Chowdhury, F. Meirer, B. M. Weckhuysen, J. Gascon, *Nat. Catal.* **1**, 398–411 (2018).
18. K. Cheng *et al*., *Chem* **3**, 334–347 (2017).
19. Q. N. Wang *et al*., *ACS Catal.* **9**, 7204–7216 (2019).
20. A. Maneffa, P. Priecel, J. A. Lopez-Sanchez, *ChemSusChem* **9**, 2736–2748 (2016).
21. C. L. Williams *et al*., *ACS Catal.* **2**, 935–939 (2012).
22. G. Lopez, M. Artetxe, M. Amutio, J. Bilbao, M. Olazar, *Renew. Sustain. Energy Rev.* **73**, 346–368 (2017).
23. A. Inaba, T. Kashiwagi, *Macromolecules* **19**, 2412–2419 (1986).
24. B. Behera, S. S. Ray, I. Singh, in *Fluid Catalytic Cracking VII: Materials, Methods and Process Innovations*, M. L. Occelli, Ed. (Elsevier, 2007), pp. 163–200.
25. S. Luo, S. C. Ho, M. M. Wu, in *Synthetics, Mineral Oils, and Bio-Based Lubricants: Chemistry and Technology*, L. R. Rudnick, Ed. (CRC Press, 2020), pp. 161–180.
26. R. Ahuja *et al*., *Nat. Chem.* **3**, 167–171 (2011).
27. H. B. Mostad, T. U. Riis, O. H. Ellestad, *Appl. Catal.* **63**, 345–364 (1990).
28. Q. L. Zhu, Q. Xu, *Energy Environ. Sci.* **8**, 478–512 (2015).
29. S. Pradhan *et al*., *Chem. Sci.* **3**, 2958–2964 (2012).
30. S. E. Stein, R. L. Brown, "Structures and Properties Group Additivity Model," in NIST Chemistry WebBook, NIST Standard Reference Database Number 69, P. J. Linstrom, W. G. Mallard, Eds.; https://doi.org/10.18434/T4D303.
31. D. W. Flaherty, E. Iglesia, *J. Am. Chem. Soc.* **135**, 18586–18599 (2013).
32. C. Xu, Y. L. Tsai, B. E. Koel, *J. Phys. Chem.* **98**, 585–593 (1994).
33. J. L. Carter, J. A. Cusumano, J. H. Sinfelt, *J. Catal.* **20**, 223–229 (1971).
34. F. Zhang, M. Zeng, R. D. Yappert, J. Sun, Y.-H. Lee, A. M. LaPointe, B. Peters, M. M. Abu-Omar, S. L. Scott, Data deposited in the Dryad repository: https://doi.org/10.25349/D9ZG6B.

ACKNOWLEDGMENTS

We thank D. Uchenik and S. Walker for their assistance in FD-MS and NMR experiment setup and data collection. **Funding:** Supported by award DE-AC-02-07CH11358 from the U.S. Department of Energy, Office of Basic Energy Sciences, Division of Chemical Sciences, Geosciences, and Biosciences, as a subcontract from Ames Laboratory. Some experiments were performed using the MRL Shared Experimental Facilities, supported by the MRSEC Program of the NSF under award DMR 1720256, a member of the NSF-funded Materials Research Facilities Network (www.mrfn.org). **Author contributions:** F.Z., M.Z., and S.L.S. designed the experiments and wrote the manuscript. F.Z. and M.Z. were assisted by J.S. and Y.-H.L. in performing experiments and analyzing data. R.D.Y. performed the modeling and assisted with data analysis. A.M.L. analyzed molecular weights. A.M.L., B.P., and M.M.A.-O. provided experimental and theoretical guidance and edited the manuscript. **Competing interests:** F.Z., M.Z., M.M.A.-O., and S.L.S. are inventors on U.S. patent application 63/052,277 (UC Santa Barbara, filed 7/15/2020) partially based on this work. All other authors declare that they have no competing interests. **Data and materials availability:** Data supporting the findings of this study are presented in the paper and the supplementary materials. Additional raw data related to this paper (DSC, FD-MS, GC-FID, GC-TCD, GPS, NMR, computational model fits) are available in the Dryad repository (*34*).

SUPPLEMENTARY MATERIALS

science.sciencemag.org/content/370/6515/437/suppl/DC1
Materials and Methods
Figs. S1 to S16
Tables S1 to S7
References (*35*–*39*)

29 April 2020; accepted 18 August 2020
10.1126/science.abc5441

Science

Polyethylene upcycling to long-chain alkylaromatics by tandem hydrogenolysis/ aromatization

Fan ZhangManhao ZengRyan D. YappertJiakai SunYu-Hsuan LeeAnne M. LaPointeBaron PetersMahdi M. Abu-OmarSusannah L. Scott

Science, 370 (6515), • DOI: 10.1126/science.abc5441

A new future for polyethylene

Most current plastic recycling involves chopping up the waste and repurposing it in materials with less stringent engineering requirements than the original application. Chemical decomposition at the molecular level could, in principle, lead to higher-value products. However, the carbon-carbon bonds in polyethylene, the most common plastic, tend to resist such approaches without exposure to high-pressure hydrogen. F. Zhang *et al.* now report that a platinum/alumina catalyst can transform waste polyethylene directly into long-chain alkylbenzenes, a feedstock for detergent manufacture, with no need for external hydrogen (see the Perspective by Weckhuysen).

Science, this issue p. 437; see also p. 400

Science (ISSN 1095-9203) is published by the American Association for the Advancement of Science. 1200 New York Avenue NW, Washington, DC 20005. The title *Science* is a registered trademark of AAAS.